Metal-Assisted Unusual Hydroxylation at the Carbon Atom of the Triazine Ring in Dinuclear Ruthenium(II) and Osmium(II) Complexes Bridged by 2,4,6-Tris(2-pyridyl)-1,3,5-triazine: Synthesis, Structural Characterization, Stereochemistry, and Electrochemical Studies

Parimal Paul,*,† Beena Tyagi, Anvarhusen K. Bilakhiya, Parthasarathi Dastidar, and Eringathodi Suresh

Discipline of Silicates and Catalysis, Central Salt and Marine Chemicals Research Institute, G. B. Marg, Bhavnagar-364 002, India

Received August 5, 1999

The reaction of *cis*-$[M(bpy)_2Cl_2]$ (M = Ru(II), and Os(II)) with 2,4,6-tris(2-pyridyl)-1,3,5-triazine (tptz) in refluxing ethanol−water resulted in the formation of dinuclear complexes of the composition $[\{M(bpy)_2\}_2(tptz\text{-}OH)](PF_6)_3 \cdot nH_2O$ ($n = 1$ for Ru and $n = 0$ for Os). In this reaction an unusual metal-induced hydroxylation at the carbon atom of the triazine ring of bridged tptz occurred. However, hydroxylation did not occur in the corresponding mononuclear complexes under similar reaction condition. A comparative study revealed that sufficient electrophilicity on the carbon atom and free movement of the attached pyridyl ring promoted the hydroxylation reaction. The hydroxylated dinuclear complexes exist in two stereoisomeric forms, a *rac* form ($\Delta\Delta/\Lambda\Lambda$) and a *meso* form ($\Delta\Lambda/\Lambda\Delta$). Both diastereoisomers have been isolated in pure form and characterized. The molecular structures of the *rac* form of Ru(II) complex (**3-II**) and *meso* form of the Os(II) complex (**4-I**) have been established by single-crystal X-ray studies. Crystal data: complex **3-II**, monoclinic, $C2/c$, $a = 24.584(7)$ Å, $b = 14.309(4)$ Å, $c = 41.044(13)$ Å, $\beta = 92.84(2)°$, $V = 14420.0(7)$ Å^3, $Z = 8$, $R = 0.179$, wR2 = 0.479; complex **4-I**, triclinic, $P\bar{1}$, $a = 13.444(7)$ Å, $b = 14.576(5)$ Å, $c = 19.641(7)$ Å, $\alpha = 98.21(3)°$, $\beta = 101.67(4)°$, $\gamma = 105.80(4)°$, $V = 3546.0(3)$ Å^3, $Z = 2$, $R = 0.093$, wR2 = 0.279. The poor data quality of **3-II** did not allow anisotropic refinement of non-hydrogen atoms except Ru and P. A PLUTO drawing of this compound is given only to support the molecular structure. ^{1}H NMR data have been used to characterize the diastereoisomers. The dinuclear complexes exhibit unusual electrochemical behavior; cathodic shifts of the metal-centered oxidations and ligand-based first reduction compared to mononuclear complexes have been observed. There is a splitting in the metal-centered oxidation potentials, indicating strong electronic communication between the metal centers. Comproportionation constants (K_{com}) of the mixed-valence species have been calculated; the values are in the range 6.03×10^4−4.7×10^6. It appears that a metal−metal interaction occurred by an electron-transfer mode across the low-lying π^* orbital of the bridged tptz.

Introduction

In recent years, there has been tremendous growth in the field of supramolecular ruthenium(II) and osmium(II) polypyridyl complexes because of their utility in a variety of photoredox applications involving multielectron processes.[1−10] Designing of these complexes requires bridging ligands (spacers) having two or more bidentate sets of coordination sites to incorporate molecular components (building blocks) such as $[M(bpy)_2]^{2+}$ (where bpy = 2,2′-bipyridine). The ligand 2,4,6-tris(2-pyridyl)-1,3,5-triazine (tptz) is a potential spacer, which functions as a bis-bidentate or simultaneously as a tridentate and a bidentate ligand and has been used to prepare dicobalt,[11] dimercury,[12] and diruthenium[13−15] complexes.

tptz is usually stable toward hydrolysis[16] and has been used as an analytical reagent for various metal ions.[17,18] A number of transition-metal and lanthanide complexes of the same ligand have also been reported.[19−23] However, Lerner and Lippard

† E-mail: salt@bhavnagar.com.

(1) Balzani, V.; Campagna, S.; Denti, G.; Juris, A.; Serroni, S.; Venturi, M. *Acc. Chem. Res*. **1998**, *31*, 26.
(2) Venturi, M.; Serroni, S.; Juris, A.; Campagna, S.; and Balzani, V. *Top. Curr. Chem*. **1998**, *197*, 193.
(3) De Cola, L.; Belser, P. *Coord. Chem. Rev*. **1998**, *177*, 301.
(4) Ishow, E.; Gourdon, A.; Launay, J.-P.; Chiorboli, C.; Scandola, F. *Inorg. Chem*. **1999**, *38*, 1504.
(5) Reinhoudt, D. N., Ed. *Comprehensive Supramolecular Chemistry*; Pergamon: London, 1996.
(6) Balzani, V.; Juris, A.; Venturi, M.; Campagna, S.; Serroni, S. *Chem. Rev*. **1996**, *96*, 759.
(7) Lehn, J.-M.; *Supramolecular Chemistry*; VCH: Weinheim, Germany, 1995.
(8) Sauvage, J.-P.; Collin, J.-P.; Chambron, J.-C.; Guillerez, S.; Coudret, C. *Chem. Rev*. **1994**, *94*, 993.
(9) Juris, A.; Balzani, V.; Campagna, S.; Denti, G.; Serroni, S.; Frei, G.; Gudel, H. U. *Inorg. Chem*. **1994**, *33*, 1491.
(10) Belser, P.; von Zelewsky, A.; Frank, M.; Seel, C.; Vogtle, F.; De Cola, L.; Barigelletti, F.; Balzani, V. *J. Am. Chem. Soc*. **1993**, *115*, 4076.
(11) Vagg, R. S.; Warrener, R. N.; Watton, E. C. *Aust. J. Chem*. **1969**, *22*, 141.
(12) Half-penny, J.; Small, R. W. H. *Acta Crystallogr*. **1982**, *B38*, 939.
(13) Thomas, N. C.; Foley, B. L.; Rheingold, A. L. *Inorg. Chem*. **1988**, *27*, 3426.
(14) Chirayil, S.; Hegde, V.; Jahng, Y.; Thummel, R. P. *Inorg. Chem*. **1991**, *30*, 2821.
(15) Berger, R. M.; Ellis, D. D., II. *Inorg. Chim. Acta* **1996**, *241*, 1.
(16) Smolin, E. M.; Rapoport, L. S. *Triazines and Derivatives*; Interscience: New York, 1959; p 163.
(17) Embry, W. A.; Ayres, G. H. *Anal. Chem*. **1968**, *40*, 1499.
(18) Janmohamed, M. J.; Ayres, G. H. *Anal. Chem*. **1972**, *44*, 2263.

10.1021/ic990938x CCC: $19.00
Published on Web 12/17/1999

found for the first time that Cu(II) in aqueous media promoted the hydrolysis of tptz to the bis(2-pyridylcarbonyl)amide anion (bpca);[24,25] crystallographic characterizations of Cu(II) complexes with hydrolyzed tptz were also reported.[26,27] Subsequently, Thomas et al.[13] have reported a photoinduced methoxylation at the triazine ring, which occurred during the reaction of $[Ru(CO)_2Cl_2]$ with tptz in methanol and resulted in the formation of $\{\mu\text{-}C_3N_3(OMe)(py)_2(pyH)\}[Ru(CO)_2Cl_2]_2$. However, no methoxylation occurred when the same reaction was carried out in dark. Recently, we reported the rhodium chemistry of tptz;[28−30] Rh(III) in ethanol−water promoted the hydrolysis of tptz to bpca. However, with a judicious choice of solvent and reaction conditions, we were also able to prepare Rh(III) complexes of intact tptz.[29]

We were interested in exploring the chemistry of dinuclear Ru(II) and Os(II) complexes of tptz. Interestingly, we observed that during the reaction of tptz with the building blocks *cis*-$[Ru(bpy)_2Cl_2]$/*cis*-$[Os(bpy)_2Cl_2]$ in ethanol−water, an unusual hydroxylation of tptz occurred. It may be noted that, in the case of dinuclear Ru(II) complex, our observation is different from that of Berger and Ellis,[15] who reported a complex of the molecular formula $[\{Ru(bpy)_2\}_2tptz](PF_6)_4$ obtained by the reaction of tptz with *cis*-$[Ru(bpy)_2Cl_2]$ under similar reaction conditions. Mononuclear complexes of Ru(II) and Os(II) of tptz and the asymmetric dinuclear complex $[(bpy)_2Ru\text{-}tptz\text{-}Ru(tpy)]^{4+}$ have also been synthesized in order to compare their properties to that of hydroxylated dinuclear complexes to understand mechanistic aspects of the hydroxylation and electrochemical behavior. Herein, we report the synthesis, structural and spectroscopic characterization, stereochemistry, mechanistic aspects of the hydroxylation, and electrochemical behavior of these novel complexes.

Experimental Section

Materials. The ligand 2,4,6-tris(2-pyridyl)-1,3,5-triazine (tptz), 2,2′-bipyridine (bpy), 2,2′:6′,2″-terpyridine (tpy), ammonium hexafluorophosphate, tetrabutylammonium tetrafluoroborate, ammonium hexachloroosmate, and SP Sephadex C-25 were purchased from Aldrich. Hydrated ruthenium trichloride was purchased from Arora Matthey. The complexes *cis*-$[Ru(bpy)_2Cl_2]\cdot 2H_2O$ and *cis*-$[Os(bpy)_2Cl_2]\cdot 2H_2O$ were prepared according to the literature methods.[31,32] All organic solvents were of reagent grade and were purified by standard methods before use.

Physical Measurements. Elemental analyses (C, H, and N) were performed on a model 2400 Perkin-Elmer elemental analyzer. Infrared spectra were recorded on a Perkin-Elmer spectrum GX FT-IR spectrophotometer as KBr pellets. NMR spectra were recorded on a model DPX 200 Brucker FT-NMR Instrument. The UV/vis spectra were recorded on a model 8452A Hewlett-Packard diode array spectrophotometer. Electrochemical measurements were made using CHI 660A electrochemical workstation equipment. Cyclic and square wave voltametries were carried out in a three-electrode cell consisted of a glassy-carbon working electrode, a platinum-wire auxiliary electrode, and a SCE reference electrode. Solutions of the complexes in purified acetonitrile containing 0.1 M tetrabutylammonium tetrafluoroborate as supporting electrolyte were deaerated by bubbling nitrogen for 20 min prior to each experiment.

Synthesis of Metal Complexes. $[(bpy)_2Ru(tptz)](PF_6)_2\cdot H_2O$ (1). This complex was prepared by the method of Thummel et al.[14] but purified by a different procedure. The complex *cis*-$[Ru(bpy)_2Cl_2]\cdot 2H_2O$ (0.26 g, 0.5 mmol) and tptz (0.156 g, 0.5 mmol) were taken up in ethanol−water (1:1, 40 mL), and the reaction mixture was refluxed for 16 h. The solvent of the reaction mixture was evaporated to dryness, and the residue was redissolved in 5 mL of water and filtered. The filtrate was put on to a Sephadex SP C-25 column and eluted with 0.1 M aqueous NaCl solution. The solvent was removed by rotary evaporation, and the residue was extracted with dry ethanol to remove NaCl. The ethanolic solution was evaporated to dryness and redissolved in 5 mL of water, and a saturated aqueous solution (5 mL) of NH_4PF_6 was added. The dark red precipitate thus obtained was isolated by filtration, washed with water and diethyl ether, and dried in vacuo; yield 0.33 g (64%). Anal. Calcd for $C_{38}H_{30}RuN_{10}OP_2F_{12}$: C, 44.15; H, 2.93; N, 13.55. Found: C, 43.97; H, 2.92; N, 13.35. ^{1}H NMR (δ (ppm), CD_3CN): 6.83 (t, 1H), 7.01 (d, 1H), 7.10−7.17 (m, 2H), 7.24 (t, 1H), 7.28−7.70 (m, 9H), 7.80−8.16 (m, 5H), 8.19−8.30 (m, 2H), 8.36−8.52 (m, 3H), 8.73 (d, 1H), 8.88 (d, 1H), 8.99 (d, 1H), 9.18 (d, 1H). UV/vis (CH_3CN; λ_{max}, nm (ϵ)): 492 (7.8×10^3), 432 (1.2×10^4), 288 (7.3×10^4), 252 (3.3×10^4).

$[(bpy)_2Os(tptz)](PF_6)_2\cdot 2H_2O$ (2). This complex was prepared by following a procedure similar to that of complex **1**, except the reaction mixture was refluxed for 24 h; yield 0.335 g (60%). Anal. Calcd for $C_{38}H_{30}OsN_{10}OP_2F_{12}$: C, 40.65; H, 2.69; N, 12.47. Found: C, 40.80; H, 2.72; N, 12.43. ^{1}H NMR (δ (ppm), CD_3CN): 6.78 (d, 2H), 7.04−7.26 (m, 4H), 7.31−7.52 (m, 6H), 7.58−7.64 (m, 2H), 7.72−8.10 (m, 6H), 8.19 (d, 1H), 8.35 (d, 1H), 8.46 (dd, 2H), 8.70 (d, 1H), 8.80 (d, 1H), 8.87 (d, 1H), 9.10 (d, 1H). UV/vis (CH_3CN; λ_{max}, nm (ϵ)): 710 sh (2.0×10^3), 516 (1.1×10^4), 430 (1.3×10^4), 290 (7.3×10^4), 250 (3.6×10^4).

$[\{Ru(bpy)_2\}_2(tptz\text{-}OH)](PF_6)_3\cdot H_2O$ (3-I, 3-II). A mixture of *cis*-$[Ru(bpy)_2Cl_2]\cdot 2H_2O$ (0.52 g, 1 mmol) and tptz (0.156 g, 0.5 mmol) was refluxed in ethanol−water (2:1, 45 mL) for 24 h. The volume of the solution was reduced to ca. 10 mL by rotary evaporation and chromatographed on a Sephadex SP C-25 column using 0.1 M followed by 0.2 M aqueous NaCl solution as eluent. A small fraction was obtained with 0.1 M NaCl solution, but the major band (desired fraction) was eluted with 0.2 M NaCl solution. The solvent of the desired fraction was evaporated to dryness, redissolved in dry ethanol (15 mL), and filtered to remove NaCl. The solvent of the filtrate was removed, the residue was dissolved in water (5 mL), and a saturated aqueous solution of NH_4PF_6 was added. The dark red precipitate thus obtained was isolated by filtration and washed with water and diethyl ether. The compound was then dissolved in 10 mL of acetonitrile, 10 mL of 1,4-dioxane was added slowly, and the solution was allowed to undergo slow evaporation at room temperature. After 7 days, diamond-shaped dark red crystals (**3-I**) together with a few long needle-shaped (thin) crystals were separated. The compound was isolated at this stage by filtration, and the filtrate was kept at room temperature allowing slow evaporation. After 5 days long needle-shaped crystals (**3-II**) were separated, which were isolated by filtration. Each isomer was recrystallized three times by following the same procedure as described above. This treatment yielded pure complexes of **3-I** and **3-II**, yield 0.27 g for **3-I** (34%) and 0.18 g for **3-II** (22%) (total 56%). Data for **3-I**: Anal. Calcd for $C_{58}H_{47}Ru_2N_{14}O_2P_3F_{18}$: C, 43.29; H, 2.94; N, 12.19. Found: C, 42.94; H, 2.96; N, 12.28. ^{1}H NMR (δ (ppm), CD_3CN): 5.28 (s, 1H), 6.72 (d, 1H), 6.77 (d, 2H), 6.92−7.01 (m, 2H), 7.06 (d, 1H), 7.16−7.49 (m, 13H), 7.55 (t, 2H), 7.62−8.05 (m, 15H), 8.20−8.33

(19) Fraser, F. H.; Epstein, P.; Macero, D. J. *Inorg. Chem.* **1972**, *11*, 2031.
(20) Tokel-Takvoryan, N. E.; Hwmingway, R. E.; Bard, A. J. *J. Am. Chem. Soc.* **1973**, *95*, 6582.
(21) Arif, A. M.; Hart, F. A.; Hursthouse, M. B.; Thornton-Pett, M.; Zhu, W. *J. Chem. Soc., Dalton Trans.* **1984**, 2449.
(22) Chan, G. Y. S.; Drew, M. G. B.; Hudson, M. J.; Isaacs, N. S.; Byers, P.; Madic, C. *Polyhedron* **1996**, *15*, 3385.
(23) Gelling, A.; Olsen, M. D.; Orrell, K. G.; Osborne, A. G.; Sik, V. *J. Chem. Soc., Chem. Commun.* **1997**, 587.
(24) Lerner, E. I.; Lippard, S. J. *J. Am. Chem. Soc.* **1976**, *98*, 5397.
(25) Lerner, E. I.; Lippard, S. J. *Inorg. Chem.* **1977**, *16*, 1546.
(26) Cantarero, A.; Amigo, J. M.; Faus, J.; Julve, M.; Debaerdemaeker, T. *J. Chem. Soc., Dalton Trans.* **1988**, 2033.
(27) Faus, J.; Julve, M.; Amigo, J. M.; Debaerdemaeker, T. *J. Chem.* Soc., *Dalton Trans.* **1989**, 1681.
(28) Paul, P.; Tyagi, B.; Bhadbhade, M. M.; Suresh, E. *J. Chem. Soc., Dalton Trans.* **1997**, 2273.
(29) Paul, P.; Tyagi, B.; Bilakhiya, A. K.; Bhadbhade, M. M.; Suresh, E.; Ramachandraiah, G. *Inorg. Chem.* **1998**, *37*, 5733.
(30) Paul, P.; Tyagi, B.; Bilakhiya, A. K.; Bhadbhade, M. M.; Suresh, E. *J. Chem. Soc., Dalton Trans.* **1999**, 2009.
(31) Sullivan, B. P.; Salmon, D. J.; Meyer, T. J. *Inorg. Chem.* **1978**, *17*, 3334.
(32) Kober, E. M.; Caspar, J. V.; Sullivan, B. P.; Meyer, T. J. *Inorg. Chem.* **1988**, *27*, 4587.

Table 1. Summary of Crystallographic Data for Complexes **4-I** and **3-II**

	4-I	**3-II**
chem formula	$C_{58}H_{45}F_{18}N_{14}OOs_2P_3$	$C_{58}H_{47}F_{18}N_{14}O_2Ru_2P_3$
fw	1769.39	1609.15
a (Å)	13.444(7)	24.584(7)
b (Å)	14.576(5)	14.309(4)
c (Å)	19.641(7)	41.044(13)
α (deg)	98.21(3)	90.0
β (deg)	101.67(4)	92.84(2)
γ (deg)	105.80(4)	90.0
Z	2	8
V (Å^3)	3546(3)	14 420(7)
space group	triclinic, $P\bar{1}$	monoclinic, *C*2/*c*
radiation used, *λ* (Å)	Mo Kα, 0.7107	Mo Kα, 0.7107
ρ_{calcd} (g cm^{-3})	1.657	1.482
abs coeff, *μ* (cm^{-1})	3.743	0.581
temp (K)	295	295
final $R(F_o^2)^a$	0.093	0.179
weighted $R(F_o^2)^b$	0.259	0.479

^{a} R1 = $\sum||F_o| - |F_c||/\sum|F_o||$. ^{b} wR2 = $[\sum w(F_o^2 - F_c^2)^2/\sum w(F_o^2)^2]^{1/2}$.

(m, 5H), 8.46 (d, 1H), 8.79 (d, 2H), 8.81 (d, 2H). UV/vis (CH_3CN; λ_{max}, nm (ϵ)): 586 (7.0×10^3), 460 (2.2×10^4), 334 (1.9×10^4), 290 (9.1×10^4), 244 (4.4×10^4). Data for **3-II**: Anal. Calcd for $C_{58}H_{47}Ru_2N_{14}O_2P_3F_{18}$: C, 43.29; H, 2.94; N, 12.19. Found: C, 43.04; H, 2.87; N, 12.10. ^{1}H NMR (δ (ppm), CD_3CN): 5.96 (d, 1H), 6.30 (t, 1H), 6.48 (s, 1H), 6.52 (m, 1H), 6.75 (d, 1H), 6.96 (d, 2H), 7.05 (t, 2H), 7.12−7.20 (m, 4H), 7.30−7.37 (m, 4H), 7.47 (d, 2H), 7.59−7.70 (m, 8H), 7.91−7.80 (m, 6H), 8.00−8.18 (m, 4H), 8.32 (d, 2H), 8.42 (d, 2H), 8.88 (d, 2H), 9.40 (d, 2H). UV/vis (CH_3CN; λ_{max}, nm (ϵ)): 582 (7.7×10^3), 460 (2.0×10^4), 334 (1.9×10^4), 290 (9.2×10^4), 244 (4.3×10^4).

[{Os(bpy)$_2$}$_2$(tptz-OH)](PF$_6$)$_3$ (4-I, 4-II). These complexes were synthesized by the reaction of *cis*-$[Os(bpy)_2Cl_2]\cdot 2H_2O$ (0.61 g, 1 mmol) and tptz (0.156 g, 0.5 mmol) by following a procedure similar to that of complexes **3-I** and **3-II**, except the reaction mixture was refluxed for 36 h, yield 0.28 g (32%) for **4-I** (isomer-I, diamond-shaped crystals) and 0.18 g (20%) for **4-II** (isomer-II, needle-shaped crystals) (total 52%). Data for **4-I**: Anal. Calcd for $C_{58}H_{45}Os_2N_{14}OP_3F_{18}$: C, 39.37; H, 2.56; N, 11.08. Found: C, 39.06; H, 2.41; N, 11.01. ^{1}H NMR (δ (ppm), CD_3CN): 5.34 (s, 1H), 6.57 (d, 1H), 6.71 (t, 1H), 6.86−6.93 (m, 5H), 7.07−7.21 (m, 10H), 7.33−7.43 (m, 6H), 7.57−7.75 (m, 10H), 7.80−7.85 (m, 3H), 7.98 (t, 1H), 8.20−8.31 (m, 4H), 8.43 (d, 1H), 8.71 (d, 2H). UV/vis (CH_3CN; λ_{max}, nm (ϵ)): 740 (9.1×10^3), 495 sh (2.1×10^4), 466 (2.3×10^4), 340 (2.0×10^4), 292 (9.2×10^4), 244 (4.5×10^4). Data for **4-II**: Anal. Calcd for $C_{58}H_{45}Os_2N_{14}OP_3F_{18}$: C, 39.37; H, 2.56; N, 11.08. Found: C, 39.41; H, 2.68; N, 10.95. ^{1}H NMR (δ (ppm), CD_3CN): 6.02 (d, 1H), 6.37 (t, 1H), 6.53 (s, 1H), 6.55 (m, 1H), 6.77−6.84 (m, 3H), 6.94−7.12 (m, 6H), 7.22 (t, 2H), 7.35−7.49 (m, 8H), 7.63−7.94 (m, 14H), 8.31 (d, 2H), 8.41 (d, 2H), 8.80 (d, 2H), 9.16 (d, 2H). UV/vis (CH_3CN; λ_{max}, nm (ϵ)): 732 (9.2×10^3), 498 sh (1.9×10^4), 466 (2.2×10^4), 342 (1.9×10^4), 294 (9.2×10^4), 244 (4.3×10^4).

[(bpy)$_2$Ru(tptz)Ru(tpy)](PF$_6$)$_4$ (5). This complex was prepared by the method of Thummel et al.[14] Anal. Calcd for $C_{53}H_{39}Ru_2N_{13}P_4F_{24}$: C, 38.82; H, 2.40; N, 11.10. Found: C, 38.56; H, 2.57; N, 11.02. ^{1}H NMR (δ (ppm), CD_3CN): 7.00−7.14 (m, 3H), 7.24−7.46 (m, 5H), 7.69−7.91 (m, 11H), 8.01−8.20 (m, 9H), 8.35−8.63 (m, 9H), 8.76−8.82 (m, 1H), 9.06 (d, 1H). UV/vis (CH_3CN; λ_{max}, nm (ϵ)): 478 (2.3×10^4), 312 (5.0×10^4), 290 (7.1×10^4), 274 (7.3×10^4), 234 (4.9×10^4).

Crystal Structure Determination of Complexes 3-II and 4-I. Crystals of complexes **3-II** and **4-I** were grown from acetonitrile−1,4-dioxane (1:1) solution by slow evaporation at room temperature. A summary of crystallographic details is given in Table 1. Both structures were solved by the Patterson method, and all the non-hydrogen atoms could be located by subsequent difference Fourier syntheses. For complex **3-II**, Ru and P atoms were refined anisotropically. Poor data quality did not allow anisotropic refinement for the rest of the non-hydrogen atoms. We did not observe any disorder in PF_6^-; one PF_6^- occupies a general position whereas the other two are residing on a special position (2-fold). A PLUTO drawing of this complex is presented only to support the molecular structure and its stereochemistry. In the case of complex **4-I** all non-hydrogen atoms, except N(7), were refined anisotropically. All F atoms of PF_6^- anions appears severally disordered. In two PF_6^- anions, F atoms were disordered over 12 positions whereas, in the other PF_6^- anion, they were disordered over 16 positions. Occupancy factors for all the fluorine atoms were assigned on the basis of their peak heights. H atoms were fixed stereochemically and refined using the riding model. After anisotropic refinement, several unaccounted electron density peaks ranging from 2.98 to 1.12 e/Å^3 were observed in the final difference Fourier map, and almost all of them have short contacts with Os; this could be due to the absorption problem which could not be corrected as no suitable reflections were found for empirical absorption correction.

Programs used: CAD4 PC[33] for crystal orientation, unit cell refinement, and intensity data measurement; NRCVAX[34] for LP correction and data reduction; SHELX-97[35] for structure solution and full-matrix least-squares refinement. Graphics: ORTEP-II[36] and PLUTO.[37] Calculations of molecular geometry: CSU.[38] All computations were performed on a Pentium-Pro PC.

Results and Discussion

Synthesis of the Complexes. Mononuclear complexes $[(bpy)_2Ru(tptz)](PF_6)_2\cdot H_2O$ (**1**) and $[(bpy)_2Os(tptz)](PF_6)\cdot 2H_2O$ (**2**) were prepared by the reaction of *cis*-$[M(bpy)_2Cl_2]\cdot 2H_2O$ (M = Ru(II), Os(II)) and tptz in refluxing ethanol−water (1:1). Complex **1**, however, was reported earlier with inadequate characterization data.[14,39] Both **1** and **2** were purified by column chromatography on Sephadex-SP C-25 and isolated as the PF_6^- salt. The dinuclear complexes were synthesized by the reaction of *cis*-$[M(bpy)_2Cl_2]\cdot 2H_2O$ with tptz in a 2:1 mole ratio in refluxing ethanol−water. After purification of these complexes by column chromatography on Sephadex, the ^{1}H NMR spectra of both the complexes revealed an unprecedented hydroxylation of the triazine ring of tptz and also the presence of two isomeric species. We separated the isomers of both complexes by partial crystallization in acetonitrile−1,4-dioxane (1:1) mixture. The first fraction of the Ru complex gave dark red diamond-shaped crystals of the composition $[\{Ru(bpy)_2\}_2(tptz\text{-}OH)](PF_6)_3\cdot H_2O$ (**3-I**), and the second fraction yielded long needle-shaped crystals of same composition (**3-II**). The first fraction of the Os complex gave dark olive green crystals of diamond shape having composition $[\{Os(bpy)_2\}_2(tptz\text{-}OH)](PF_6)_3$ (**4-I**), whereas the second fraction yielded thin long needle-shaped crystals of same composition (**4-II**). The molecular structures of complexes **3-II** and **4-I** were determined by single-crystal X-ray studies. The crystals of **3-I** were of large size but showed weak diffraction and the structure could not be solved. Crystals of **4-II** were thin, and we were unsuccessful in finding a suitable crystal for structure determination. Complex **5**, $[(bpy)_2Ru(tptz)Ru(tpy)](PF_6)_4$, was prepared by the method reported by Thummel et al.[14] However, no characterization data, except the ^{1}H NMR

(33) Gabe, E. I.; Le Page, Y.; Charland, I. P.; Lee, F. L.; White, P. S. *J. Appl. Crystallogr.* **1989**, *22*, 384.
(34) Sheldrick, G. M. *Acta Crystallogr.* **1990**, *A46*, 467.
(35) Sheldrick, G. M. *SHELX-97 Program for refinement of crystal structures*; University of Gottingen: Gottingen, Germany, 1997.
(36) Johnson, C. K. *ORTEP II*; Report ORNL-5138; Oak Ridge National Laboratory: Oak Ridge, TN, 1976.
(37) Motherwell, W. D. S.; Clegg, W. *PLUTO Program for Plotting Molecular and Crystal Structures*; University of Cambridge: Cambridge, England, 1978.
(38) Vickovic, I. *Crystal Structure Utility* (*CSU*), *a Highly Automated Program for the Calculation of Geometrical Parameters in the Crystal Structure Analysis*; Faculty of Science, University of Zagreb: Zagreb, Yugoslavia, 1988.
(39) Berger, R. M.; Holcombe, J. R. *Inorg. Chim. Acta* **1995**, *232*, 217.

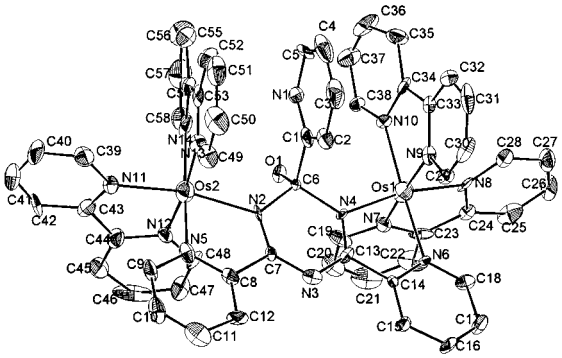

Figure 1. ORTEP view (50% probability) with atom-labeling scheme of complex **4-I**. Hydrogen atoms are omitted for clarity.

Table 2. Selected Bond Lengths (Å) and Angles (deg) for the Complex **4-I**

Os(1)−N(4)	2.105(11)	Os(2)−N(2)	2.107(11)
Os(1)−N(6)	2.092(11)	Os(2)−N(5)	2.058(14)
Os(1)−N(7)	2.082(12)	Os(2)−N(11)	2.056(13)
Os(1)−N(8)	2.056(12)	Os(2)−N(12)	2.075(12)
Os(1)−N(9)	2.060(11)	Os(2)−N(13)	2.072(13)
Os(1)−N(10)	2.063(12)	Os(2)−N(14)	2.079(14)
C(6)−O(1)	1.370(17)	N(3)−C(7)	1.302(18)
C(6)−N(2)	1.500(17)	N(3)−C(13)	1.369(19)
C(6)−N(4)	1.514(16)	N(4)−C(13)	1.304(18)
N(2)−C(7)	1.296(18)		

N(8)−Os(1)−N(9)	95.5(4)	N(11)−Os(2)−N(5)	95.6(4)
N(8)−Os(1)−N(10)	90.0(3)	N(11)−Os(2)−N(13)	96.2(4)
N(9)−Os(1)−N(10)	79.6(5)	N(5)−Os(2)−N(13)	93.4(4)
N(8)−Os(1)−N(7)	77.8(5)	N(11)−Os(2)−N(12)	78.1(5)
N(9)−Os(1)−N(7)	172.7(3)	N(5)−Os(2)−N(12)	90.5(4)
N(10)−Os(1)−N(7)	97.5(3)	N(13)−Os(2)−N(12)	173.4(4)
N(8)−Os(1)−N(6)	92.3(3)	N(11)−Os(2)−N(14)	86.1(4)
N(9)−Os(1)−N(6)	92.8(4)	N(5)−Os(2)−N(14)	173.4(4)
N(10)−Os(1)−N(6)	172.2(3)	N(13)−Os(2)−N(14)	80.1(6)
N(7)−Os(1)−N(6)	90.2(3)	N(12)−Os(2)−N(14)	96.1(4)
N(8)−Os(1)−N(4)	169.1(3)	N(11)−Os(2)−N(2)	168.8(4)
N(9)−Os(1)−N(4)	90.1(3)	N(5)−Os(2)−N(2)	76.7(5)
N(10)−Os(1)−N(4)	100.3(3)	N(13)−Os(2)−N(2)	92.5(4)
N(7)−Os(1)−N(4)	97.0(3)	N(12)−Os(2)−N(2)	93.7(3)
N(6)−Os(1)−N(4)	78.0(4)	N(14)−Os(2)−N(2)	102.4(3)
C(1)−C(6)−O(1)	110.5(12)	N(2)−C(6)−N(4)	110.2(11)
C(1)−C(6)−N(4)	108.0(11)	N(2)−C(6)−O(1)	110.1(11)
C(1)−C(6)−N(2)	109.0(11)	N(4)−C(6)−O(1)	108.9(11)

spectra of the complex containing bpy-d_8 ligands, $[(bpy\text{-}d_8)_2Ru(tptz)Ru(tpy\text{-}d_{11})]^{4+}$, has been reported. Analytical (C, H, and N) and ^{1}H NMR data of all these complexes are given in the Experimental Section. Complexes **1** and **5** have been reported earlier, but we prepared these complexes for a comparison of their properties to that of hydroxylated dinuclear complexes. This might help to elucidate mechanistic aspects of the hydroxylation and unusual electrochemical behavior of the dinuclear complexes (discussed later). It may be noted that the dinuclear Ru(II) complexes, **3-I** and **3-II**, were prepared by following the procedure of Berger and Ellis,[15] who have reported this complex as $[\{Ru(bpy)_2\}(tptz)](PF_6)_4$.

Crystal Structure. Complex 4-I. A perspective view (ORTEP) of the cation of complex **4-I** with the atom numbering is shown in Figure 1; selected bond distances and angles are given in Table 2. In this complex the bridging tptz functions as a bis-bidentate ligand to two Os(II) centers. Two bpy ligands and a bidentate coordination set of tptz formed a distorted octahedral geometry around each metal ion. An unprecedented hydroxylation occurred at one of the carbon atoms (C(6)) of the triazine ring forming a tetrahedral geometry around C(6). The angles around C(6) are in the range 108.0(11)−110.5(11)° (Table 2), which are close to the ideal value of 109.28°. The Os−N bond distances are comparable to those reported for Os−polypyridyl complexes.[40,41] In the coordination sphere of Os(1) the least-squares plane through the atoms N(4), N(7), N(8), and N(9) (best plane) shows slight tetrahedral bias (average deviation ±0.105(4) Å), and the Os(1) ion is contained well within the plane. Around Os(2), the least-squares plane through the atoms N(2), N(11), N(12), and N(13) (best plane) also shows slight tetrahedral bias (average deviation ±0.093(4) Å), and the deviation of Os(2) from the plane is −0.040(4) Å. The source of distortion primarily comes from the bites taken by the ligands. The bite angles (average 78.38°) are significantly smaller than the ideal value of 90° because of the constraint imposed by the five-membered chelate rings. In the triazine ring the C(6)−N(2) and C(6)−N(4) bond distances are typically single-bond value (average 1.507(16) Å),[42] whereas the remaining four C−N distances (average 1.316(18) Å) are similar to the mean C−N bond distances reported for other tptz complexes.[12,43] The hyroxylated triazine ring does not show good planarity. However, the five atoms N(2), C(7), N(3), C(13), and N(4) make a good plane (average deviation ±0.025(8) Å) and behave like a delocalized pentadienide moiety; the deviation of C(6) from this least-squares plane is −0.131(18) Å. The plane of the uncoordinate pyridyl ring of the hydrolyzed tptz is almost perpendicular to the plane of the C_3N_3 ring (angle between the plane is 89.12°). The other two pyridyl rings containing the C(8)−C(12) and C(14)−N(6) atoms rotated with respect to the triazine ring by 6.86(91) and 6.42(95)°, respectively. In all pyridyl rings the $C(sp^2)-C(sp^2)$ distances are normal, and the bpy ligands show a considerable overall planarity. Stereochemistry of this complex is discussed later.

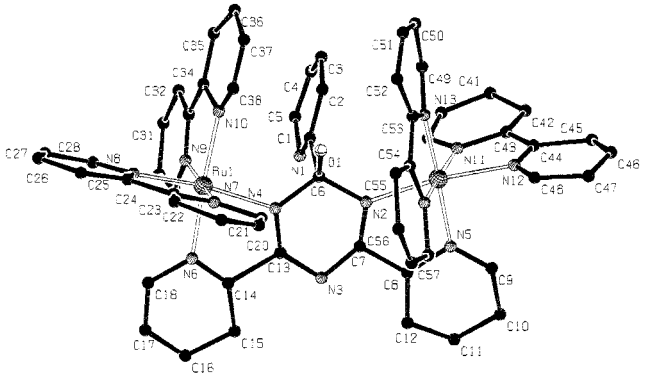

Figure 2. PLUTO drawing with atom-labeling scheme of complex **3-II**. Hydrogen atoms are omitted for clarity.

A PLUTO drawing of the cation of **3-II** is illustrated in Figure 2. This diagram is shown only to support the molecular structure. In this case also hydroxylation of tptz occurred, and its molecular structure is similar to that as found for **4-I** but with a different stereochemistry (discussed later). Bond distances and angles appears normal. A list of selected bond distances and angles is submitted as Supporting Information.

(40) Hage, R.; Haasnoot, J. G.; Nieuwenhuia, H. A.; Reedijk, J.; De Ridder, D. J. A.; Vos, J. G. *J. Am. Chem. Soc*. **1990**, *112*, 9245.
(41) Balzani, V.; Bardwell, D. A.; Barigelletti, F.; Cleary, R. L.; Guardigli, M.; Jeffery, J. C.; Sovrani, T.; Ward, M. D. *J. Chem. Soc., Dalton Trans*. **1995**, 3601.
(42) Allen, F. H.; Kennard, O.; Watson, D. G.; Brammer, L.; Orpen, A. G.; Yaylor, R. *J. Chem. Soc., Perkin Trans. 2*, **1987**, 91.
(43) Barclay, G. A.; Vagg, R. S.; Watton, E. C. *Acta Crystallogr*. **1977**, *B33*, 3487.

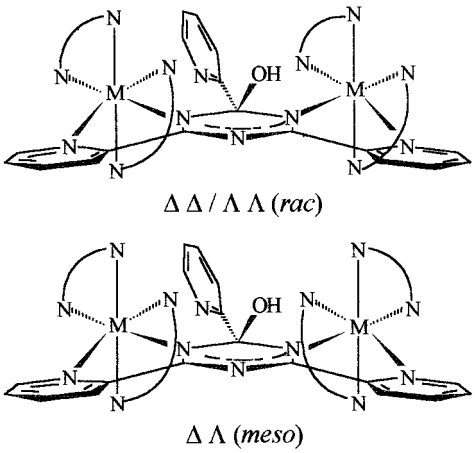

Figure 3. Diastereoisomeric forms (*rac* and *meso*) of the hydroxylated dinuclear Ru(II) and Os(II) complexes.

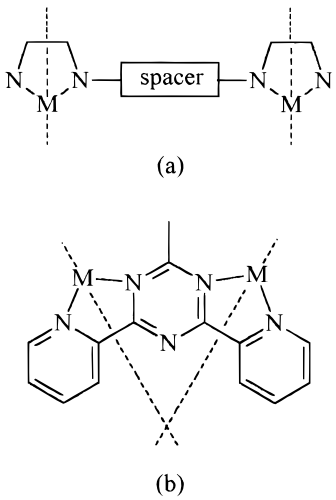

Figure 4. Axes of the bites of the bidentate moieties of the bridging ligands: (a) axes parallel; (b) axes angular.

Stereochemistry of Isomers I and II of the Dinuclear Complexes. Octahedral metal centers with bidentate ligands generally show stereoisomerism.[44] In the dinuclear complexes with symmetric bridging ligand and same terminal ligands the coordination environment of the metal centers is equivalent. In all such cases two diastereoisomeric forms ΔΛ (*meso*) and ΔΔ/ΛΛ (*rac*), as shown in Figure 3 for complexes **3** and **4**, may exist.[44−49] There is a significant difference between the *meso* and *rac* diastereoisomers as it depends on the relative orientation of the pyridyl rings with respect to the plane of the bridging ligand. In general, for complexes where the axes of the bites of the two bidentate moieties of the bridging ligand are linear or parallel (Figure 4a), the terminal polypyridyl ligands "above" and "below" the plane of the bridging ligand are approximately parallel in the ΔΔ/ΛΛ (*rac*) form, whereas they are perpendicular in the ΔΛ (*meso*) stereoisomer. But if the relationship of the axes of the two bites is angular, as in the case of tptz (Figure 4b), the above description is reversed.[44] PLUTO views

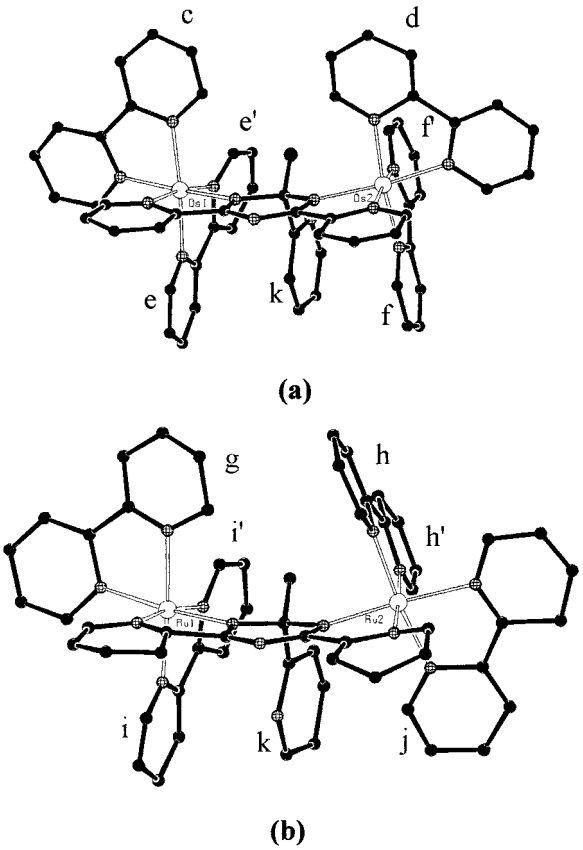

Figure 5. PLUTO view of complexes **4-I** (a, *meso*) and **3-II** (b, *rac*) showing the orientation of terminal ligands with respect to the bridging ligand. The ring-numbering scheme used for NMR discussion is also shown.

of **4-I** (isomer-**I**) and **3-II** (isomer-**II**) are shown in Figure 5. From the diagram it is clear that in **4-I** (Figure 5a) the pyridyl rings c and d are "above" the plane of the bridging ligand, and they are approximately parallel. Similarly, the pyridyl rings e and f are below the plane and approximately parallel. Therefore, isomer-**I** is the *meso* (ΔΛ/ΛΔ) form. The view of **3-II** (Figure 5b) shows the bpy ligands g and h are above the plane of the tptz and approximately perpendicular to each other. The ligands i and j (below the plane) also show a perpendicular relationship. Isomer **II**, therefore, is the *rac* (ΔΔ/ΛΛ) form.

NMR spectroscopy was found to be a useful technique to differentiate stereoisomers. The ^{1}H NMR spectra of the stereoisomers of complexes **3** and **4** were recorded in CD_3CN. The same stereoisomers of both complexes exhibit similar spectral pattern, except for a slight difference in chemical shift of some signals due to different metal ions (Ru(II) and Os(II)). The ^{1}H NMR spectra of the two isomers of the Ru complex (**3-I** and **3-II**) are shown in Figure 6. The spectra of isomer **I** (A) and isomer **II** (C) show a significant difference, which can be attributed to different orientations of the pyridyl rings. No complete assignment of the spectra could be made; however, our primary interest is in the signals of OH and some H_3 and H_6 protons which are strongly shielded/deshielded. The chemical shifts of these protons are quite informative for characterization of the diastereoisomers. Spectra A (isomer **I**) and C (isomer **II**) exhibit a singlet at 5.28 and 6.48 ppm, respectively, corresponding to one proton. For the Os complex these signals appeared at 5.34 and 6.53 ppm, respectively. These singlets disappeared after D_2O exchange, as shown in the spectra B and D of Figure 6. These singlets, therefore, can be assigned to OH, which attached to the carbon atom of the triazine ring. It is

(44) Keene, F. R. *Coord. Chem. Rev.* **1997**, *166*, 121.
(45) Ernst, S.; Kasack, V.; Kaim, W. *Inorg. Chem.* **1988**, *27*, 1146.
(46) Hage, R.; Dijkhius, A. H. J.; Haasnoot, J. G.; Prins, Rob,; Reedijk, J.; Buchanan, B. E.; Vos, J. G. *Inorg. Chem.* **1988**, *27*, 2185.
(47) Hua, X.; Zelewsky, von A. *Inorg. Chem.* **1995**, *34*, 5791.
(48) Rutherford, T. J.; Quagliotto, M. G.; Keene, F. R. *Inorg. Chem.* **1995**, *34*, 3857.
(49) Kelso, L. S.; Reitsma, D. A.; Keene, F. R. *Inorg. Chem.* **1996**, *35*, 5144.

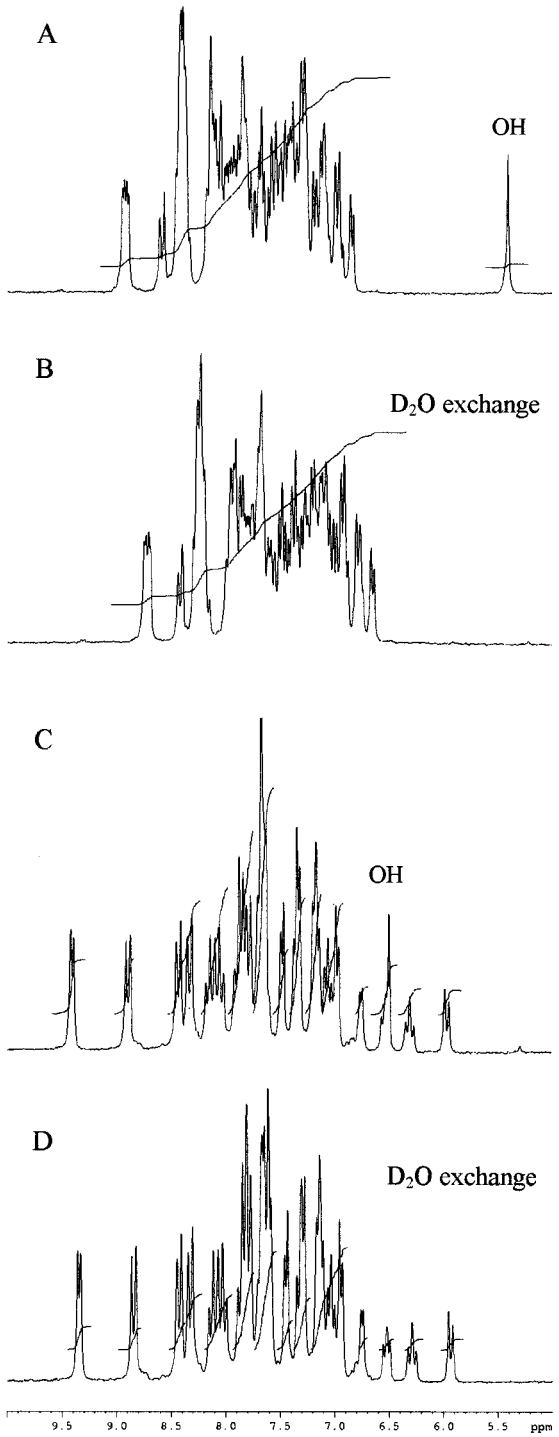

Figure 6. ^{1}H NMR spectra of **3-I** (A) and **3-II** (C) in acetonitrile-d_6. The spectra recorded after D_2O exchange (B and D) are also shown.

interesting to note that there is a significant difference in chemical shift (1.20 ppm) of the OH signals of two stereoisomers. This difference is due to the different orientations of the pyridyl ring at the vicinity of the OH. It may be noted that in Figure 5a (isomer **I** of the Os complex) the OH is being pointed directly toward the shielding face of two pyridyl rings (e′ and f′) from both sides. The distances of H of OH from the centroid of e′ and f′ rings are 3.161 and 3.973 Å, respectively. The angle ∠centroid of ring e′−N of ring e′−H of OH is 104.24°; the similar angle involving the f′ ring is 95.45°. The two rings e′ and f′ are almost parallel and at the both sides of the OH. These data suggest that the H atom of OH is in the shielding zone due to the ring current effect of both the pyridyl rings[50−52] and, therefore, strongly shielded. In the other isomer (isomer **II** of the Ru complex, Figure 5b) the H of OH experienced the shielding effect from one such pyridyl ring (i′). The other possible ring (h′) from which shielding effect may come is away from OH. This difference in shielding effect resulted in a significant difference in chemical shift of OH of the two diastereoisomer.

Another remarkable difference between the spectra A and C is that C (**3-II**, *rac*) shows four distinct resonances at 5.96 (doublet, J_{H-H} = 7.8 Hz), 6.30 (triplet), 6.52 (multiplet), and 6.75 ppm (doublet J_{H-H} = 5.4 Hz), whereas A (**3-I**, *meso*) exhibits only a doublet at 6.72 ppm (J_{H-H} = 5.4 Hz). Each of these signals corresponds to one proton. The two isomers of the Os complex (**4-I** and **4-II**) also show similar spectra. These signals are due to the protons of the uncoordinate pyridyl ring (k) of tptz. In tptz, the doublets for H_3 and H_6 have characteristic J_{H-H} values of 7.8 and 5.4 Hz, respectively.[29] Therefore, the doublets at 5.96 and 6.72 ppm in the *rac* form (C) are due to H_3 and H_6, respectively. All protons of the uncoordinated pyridyl ring in *rac* form are highly shielded; they show a upfield shifts of 2.8, 1.84, 1.19, and 2.17 ppm for H_3, H_4, H_5, and H_6, respectively (usual numbering system for pyridyl rings is used), compared to free tptz. Though the structure of **3-II** (*rac* form) is not well refined, we thought it is worth calculating the positions of these protons with respect to the surrounding pyridyl rings to find out the source of the high shielding effect. We found that the uncoordinated pyridyl ring (k) is close to the ring containing the atoms N(13) and C(49)−C(53) (h′, in Figure 5b). The H_3 of the ring k is close to the centroid of the h′ ring and well inside the shielding face. The distance of H_3 from the centroid of h′ is 2.89 Å, and the angle ∠H_3−N(13)−centroid of h′ is 76.38°, indicating that H_3 is in front of the shielding face of the h′ ring. Thus, H_3 experienced a strong shielding effect. As the distances of H_4 and H_5 from the centroid of h′ ring increases, the shielding effect decreases accordingly. However, H_6 experienced an additional shielding effect from another ring (i); therefore, it was shielded more compared to H_4 and H_5. Interestingly, in the *meso* form (Figure 5a) the nitrogen atom (N(1)) is facing the f′ ring and H_3 is at the remote side. Therefore, it is not highly shielded.

Another significant difference noted between the two spectra is in the low-field region. The *rac* form (C) exhibits four doublets at 8.32 (J_{H-H} = 8.0 Hz), 8.42 (J_{H-H} = 8.0 Hz), 8.88 (J_{H-H} = 7.8 Hz), and 9.40 ppm (J_{H-H} = 5.0 Hz); whereas the *meso* (A) form shows two overlapping doublets at 8.79 (J_{H-H} = 7.8 Hz) and 8.81 ppm (J_{H-H} = 8.0 Hz). All these signals correspond to two protons. A similar spectral pattern was also observed in the *rac* and *meso* forms of the Os complex. The *J*-values indicate that for the *rac* form the lowest field signal is due to H_6 and other three doublets are due to H_3. In the *meso* form the two lowest field doublets are assigned to H_3. In the *rac* form the bpy ligands "above"/"below" the plane of the bridging ligand are approximately perpendicular. As a result of this, the eight H_6 protons of the four bpy make four groups, two protons in each group. One such pair of H_6 falls in the desheilding plane of the neighboring bpy, and therefore, these protons are highly desheilded.

(50) Lin, C.-T.; Bottcher, W.; Chou, M.; Creutz, C.; Sutin, N. *J. Am. Chem. Soc.* **1976**, *98*, 6536.
(51) Strouse, G. F.; Schoonover, J. R.; Deusing, R.; Boyde, S.; Jones Jun W. E.; Meyer, T. J. *Inorg. Chem.* **1995**, *34*, 473.
(52) Cola L. D.; Balzani, V.; Barigelletti, F.; Flamigni, L.; Belser, P.; Zelewsky, von A.; Frank, M.; Vogtle, F. *Inorg. Chem.* **1993**, *32*, 5228.

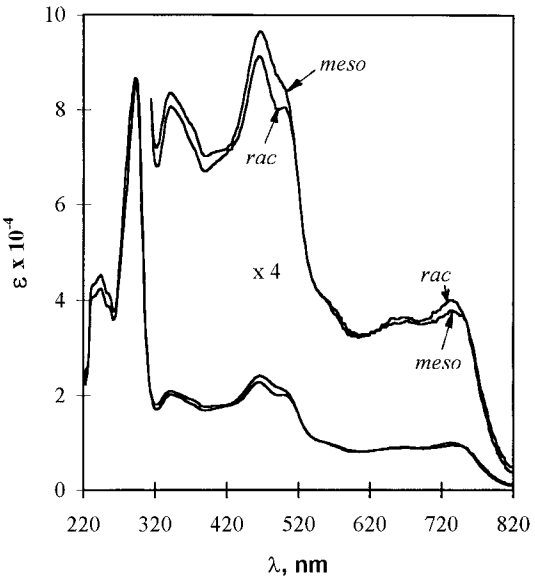

Figure 7. UV−vis spectra of **4-I** (*meso*) and **4-II** (*rac*) recorded in acetonitrile. The 314−820 nm region magnified by 4 times is also shown.

Electronic Spectra. The UV−vis spectra of all complexes were recorded in acetonitrile, and the data are presented in the Experimental Section. The low-energy bands at 492 and 432 nm of the mononuclear Ru^{II} complex (**1**) are due to metal-to-ligand charge transfer (MLCT) transitions.[28,50,51] The mononuclear Ru(II) complex of tptz, $[Ru(tptz)_2]^{4+}$, exhibits a MLCT band at 504 nm.[28] The electrochemical studies (discussed later) show that the first ligand-based reduction is associated with tptz, indicating that the lowest unoccupied molecular orbital (LUMO) is associated with the bridging ligand.[39] Therefore, the lowest energy band at 492 nm can be assigned to $d\pi \rightarrow \pi^*$(tptz), and the other band at 432 nm is due to $d\pi \rightarrow \pi^*$(bpy). The high-energy band at 288 nm is ligand-centered (LC) due to a $\pi \rightarrow \pi^*$ transition.[15,28,39] The mononuclear Os^{II} complexes (**2**) exhibits a shoulder around 700 nm and two low-energy bands at 516 and 430 nm. In a comparison of these data to that of **1** and other Os^{II} polypyridyl complexes, the shoulder around 700 nm can be assigned to a spin-forbidden MLCT transition[41] and the bands at 516 and 430 nm are due to $d\pi \rightarrow \pi^*$(tptz) and $d\pi \rightarrow \pi^*$(bpy)[51,52] MLCT transitions. The diastereoisomers of the dinuclear Ru^{II} complex, **3-I** and **3-II**, exhibit similar spectra but not same. A slight difference in λ_{max} and extinction coefficient (ϵ) is observed. A similar observation was also noted for the diastereoisomers of dinuclear Os^{II} complexes **4-I** and **4-II**, shown in Figure 7. The difference is small, but it is definite as evident from repeated experiments. It has been reported that stereochemistry has little influence on physical properties of the diastereoisomers.[53,54] However, Keene et al.[49] have reported recently that stereochemistry does influence the electronic transitions, and they reported a red shift of ~7 nm for the *rac* form compared to the *meso* form. Our studies show that stereochemistry has slight but definite influence on the electronic transition.

The spectra of mononuclear and dinuclear complexes show significant differences. The MLCT bands of the dinuclear complexes exhibit significant red shift (28 to 94 nm) compared to the corresponding mononuclear complexes. Generally, the addition of a second metal ion at the remote coordination site of the bridging ligand results in stabilization of the π^* level of the bridging ligand, leading to enhanced $d\pi \rightarrow \pi^*$ orbital overlap.[55] This effect lowers the HOMO−LUMO gap, which results in a low-energy shift of the MLCT bands in the dinuclear complexes. Therefore, our observation is consistent with other reports. It has been observed that sequential ligand-based reductions of mononuclear as well as dinuclear complexes causes gradual red shift of the MLCT bands and appearance of a new band around 340 nm, particularly for the tptz ligand.[15,39] The triazine ring of our hydroxylated dinuclear complexes contains a negative charge. Therefore, they may be considered as one-electron-reduced species. This is also supported by the fact that both the hydroxylated Ru(II) and Os(II) complexes exhibit a new band around 340 nm, as found in the one-electron-reduced species. Thus, the hydroxylated dinuclear complexes, as a one-electron-reduced species, might have also contributed to the red shift of the MLCT bands compared to mononuclear complexes. Complex **5** shows a lowest energy MLCT band at 478 nm. The high-energy ligand-centered (LC) bands ($\pi \rightarrow \pi^*$) of all complexes did not show any significant deviation in λ_{max}.

Electrochemistry. Cyclic and Osteryoung square wave voltammograms of all complexes were recorded in acetonitrile, and the data are presented in Table 3. There was little difference in peak potentials for the diastereoisomers of the dinuclear complexes. Therefore, the data for one isomer of each complex are presented. The mononuclear complexes exhibit metal-based oxidation (M(II)/M(III)) at +1.42 and +0.97 V for Ru(II) and Os(II), respectively. They show three ligand-based reductions, the first reduction of which occurs at −0.74 (for **1**) and −0.73 V (for **2**), which can be assigned to the reduction of tptz.[39] The other reduction couples are due to bpy ligands.[15,28,39] In the dinuclear complexes two metal-based oxidations and five ligand-based reductions were observed. Cyclic and Osteryoung voltammograms of **4-I** are illustrated in Figure 8. It is interesting to note that the electrochemical data of **3-I** are similar to that of the dinuclear Ru(II) complex of tptz, $[\{Ru(bpy)_2\}_2(tptz)](PF_6)_4$, reported by Berger and Ellis.[15] A remarkable similarity in electronic spectra and electrochemical data of **3-I**/**3-II** and $[\{Ru(bpy)_2\}_2(tptz)](PF_6)_4$ indicate that both are the same complex. We established the molecular geometry of **3-II** by single-crystal X-ray study, which suggest that hydroxylation in the dinuclear Ru(II) complex, reported by Berger and Ellis, also occurred.

The notable differences between the mono- and dinuclear complexes are the following: (i) The dinuclear complexes exhibit splitting of the metal-centered oxidation potentials, though the two metal centers are chemically equivalent. (ii) Metal-based oxidations occurred at significantly less positive potentials compared to mononuclear complexes. (iii) The ligand-based first reduction show a large cathodic shift (0.55 V for **3-I** and 0.50 V for **4-I**) compared to mononuclear complexes. The splitting of the metal-based oxidation potentials in symmetric dinuclear complexes indicates metal−metal electronic coupling (discussed later in detail). As we discussed earlier, the addition of a $[M(bpy)_2]^{2+}$ subunit at the remote coordination site of the bridging ligands in the homobimetallic systems results in a net stabilization of the π^* level of the bridging ligand and $d\pi$ level of the metal ions. This effect should results in an anodic shift of both metal-based oxidations and ligand-based first reduction compared to mononuclear complexes.[41,56] Interest-

(53) Ernst, S. D.; Kaim, W. *Inorg. Chem.* **1989**, *28*, 1520.
(54) Denti, G.; Campagna, S.; Serroni, S.; Ciano, M.; Balzani, V. *J. Am. Chem. Soc.* **1992**, *114*, 2944.
(55) Rillema, D. P.; Mack, K. B. *Inorg. Chem.* **1982**, *21*, 3849.
(56) Campagna, S.; Denti, G.; DeRosa, G.; Sabatino, L.; Ciano, M.; Balzani, V. *Inorg. Chem.* **1989**, *28*, 2565.

Table 3. Electrochemical Data for Mono- and Dinuclear Ruthenium(II) and Osmium Complexes in Acetonitrile Solution

	oxidation		reduction					
complex	$E_{1/2}(1)$	$E_{1/2}(2)$	$E_{1/2}(1)$	$E_{1/2}(2)$	$E_{1/2}(3)$	$E_{1/2}(4)$	$E_{1/2}(5)$	K_{com}
$[(bpy)_2Ru(tptz)](PF_6)_2 \cdot H_2O$ (**1**)	+1.42 (87)[a]		−0.74 (82)	−1.38 (96)	−1.63 (98)			
$[(bpy)_2Os(tptz)](PF_6)_2 \cdot 2H_2O$ (**2**)	+0.97 (85)		−0.73 (76)	−1.29 (92)	−1.64 (95)			
$[\{Ru(bpy)_2\}_2(tptz\text{-}OH)](PF_6)_3 \cdot H_2O$ (**3-I**)	+1.36 (98)	+0.97 (98)	−1.29 (73)	−1.37 (67)	−1.57 (65)	−1.76 (85)	−1.98 (98)	4.70×10^6
$[\{Os(bpy)_2\}_2(tptz\text{-}OH)](PF_6)_3$ (**4-I**)	+0.87 (82)	+0.58 (82)	−1.23 (88)	−1.35 (94)	−1.55 (90)	−1.78 (92)	−2.00 (90)	6.03×10^4
$[(bpy)_2Ru(tptz)Ru(tpy)](PF_6)_4$ (**5**)	+1.17 (73)	+0.86 (77)	−0.94 (71)	−1.21 (70)	−1.43 (92)	−1.64 (98)		1.86×10^5

[a] The value of ΔE_p in mV is given in the parentheses, $\Delta E_p = E_{p,a} - E_{p,c}$.

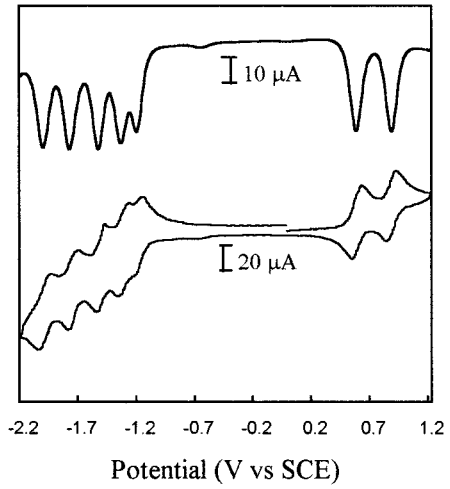

Figure 8. Osteryoung square wave and cyclic voltammograms of **4-I**, recorded in acetonitrile.

ingly, our results show a reverse trend. We observed a large cathodic shift of both metal-based oxidations and ligand-based first reduction. This unusual observation is due to hydroxylation of the triazine ring of the bridged tptz in dinuclear complexes. The hydroxylated triazine ring behaves like a pentadienide moiety, in which the added electron is delocalized over the C_2N_2 fragment of the C_3N_3 ring, the terminal nitrogen atoms of which are directly bound to metal ions. The N → M inductive effect, therefore, makes the metal centers rich in electron density, which result in cathodic shift (easy oxidation) of the metal-centered oxidation potentials. We mentioned earlier that the hydroxylated dinuclear complexes can be considered as one-electron-reduced species due to the presence of a negative charge on tptz; therefore, the addition of another electron is, in fact, the second ligand-based reduction, which obviously occurs at more negative potential. This explains the cathodic shift of the ligand-based first reduction.

In the dinuclear complexes the splitting of the metal-centered oxidations indicates metal−metal electronic interaction through the bridge.[57,58] Structural studies show that the Ru−Ru distance in **3-II** and Os−Os distance in **4-I** are 6.355 and 6.367 Å, respectively. These distances indicate that the metal centers are close enough to make electronic communication through the bridge (C_3N_3 moiety). The extent of splitting reflects the degree of metal−metal interactions. The sequential one-electron oxidations produced mixed-valence species, the stability of which can be expressed in terms of comproportionation constant, K_{com}.[45,57,59]

$$K_{com} = \exp(nF\Delta E/RT)$$

where ΔE is the difference between the two oxidation potentials in volts. The K_{com} values for the dinuclear complexes were calculated and are presented in Table 3. The K_{com} values (6.03×10^4−4.70×10^6) suggest strong electronic coupling between the metal centers, as found in the $[(NH_3)_5Ru\text{-}pz\text{-}Ru(NH_3)_5]^{5+}$ system where pz = pyrazine.[57,60] These complexes, therefore, can be considered in the Robin−Day type III catagory.[57] The metal−metal interaction via the bridge can be explained on the basis of superexchange theory,[61,62] where the overlap between metal orbitals is mediated with those of bridging ligand. The ligand tptz has a low-lying π^* orbital; therefore, in this case metal−metal communication through the bridge by an electron-transfer mode across the low-lying π^* orbital of the bridging ligand likely occurs.[58]

Mechanistic Aspects of the Hydroxylation. Triaryltriazines are usually stable toward hydrolysis.[16] However, coordination of tptz with metal ions such as Cu(II)[24] and Rh(III)[29,30] in aqueous or ethanol−water medium resulted in the hydrolysis of the ligand to bis(2-pyridylcarbonyl)amide anion. But with Ru(II), under similar reaction conditions, hydrolysis of tptz did not occur.[28] After coordination of the ligand to metal ion, the ligand-to-metal σ-donation and the π-back-bonding ability of the metal ion play a major role in the hydrolytic process.[29] The electron-withdrawing effect (L → M) leads to destabilization of the triazine ring by enhancing the electron deficiency upon it and makes the carbon atom (adjacent to the coordinated nitrogen) susceptible to nucleophilic attack. Ru(II) and Os(II) have the ability to form π-back-bonding to unsaturated ligands. This effect partially compensates the σ-electron-withdrawing effect of the metal ion, and therefore, the carbon atoms of the triazine ring are not sufficiently electropositive to interact with the nucleophiles. Therefore, nucleophilic attack by H_2O at the triazine ring of tptz in Ru(II) and Os(II) complexes was unprecedented. But it occurred in dinuclear Ru(II) and Os(II) complexes in the presence of normal laboratory light as well as in dark. Interestingly, hydroxylation did not occur in mononuclear complexes and also in asymmetrical dinuclear Ru(II) complex (**5**) under similar reaction conditions. We believe that two factors are responsible for this unusual hydroxylation reaction. These are the following: (i) sufficient electron deficiency on the carbon atom C(6); (ii) severe steric hindrance due to overcrowding of a number of pyridyl rings. The π-back-bonding ability of the metal ion partially compensates ligand-to-metal σ-electron-withdrawing effect, but at least some resultant electron deficiency makes C(6) electropositive ($C^{\delta+}$). Such effect from one metal ion may not be sufficient to make the carbon atom susceptible to necleophilic attack. However, the combined effect from both sides of the carbon atom (C(6)) by two metal ions possibly makes C(6) an electophilic center.

(57) Creutz, C. *Prog. Inorg. Chem.* **1983**, *30*, 1.
(58) Ceroni, P.; Paolucci, F.; Paradisi, C.; Juris, A.; Roffia, S.; Serroni, S.; Campagna, S.; Bard, A. J. *J. Am. Chem. Soc.* **1998**, *120*, 5480.
(59) Sutton, J. E.; Sutton, P. M.; Taube, H. *Inorg. Chem.* **1979**, *18*, 1017.
(60) Creutz, C.; Taube, H. *J. Am. Chem. Soc.* **1973**, *95*, 1086.
(61) Giuffrida, G.; Campagna, S. *Coord. Chem. Rev.* **1994**, *1355/136*, 517.
(62) Jordan, K. D.; Paddon-Row, M. N. *Chem. Rev.* **1992**, *92*, 395.

Scheme 1

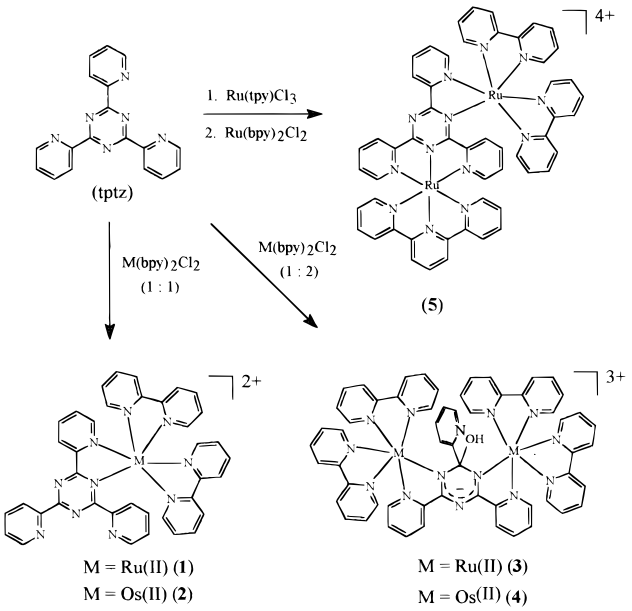

As a result, hydrolysis occurred in dinuclear complexes but not in the corresponding mononuclear complexes. The addition of OH^- to C(6) makes a tetrahedral geometry around the carbon atom. The uncoordinate pyridyl ring is also rotated to such an extent that its plane is almost perpendicular to the plane of the triazine ring. These effects (tetrahedral geometry and rotation of pyridyl ring) provide significant relief to the steric overcrowding.

In the case of complex **5**, hydroxylation did not occur, though there is a carbon atom in the triazine ring flanked between two metal-bound nitrogen atoms (Scheme 1). In this complex the pyridyl ring attached to the carbon atom to be hydroxylated is coordinated to metal ion and formed a stable five-membered planar ring in the coordination sphere. The Ru−N(pyridyl) bond rupture is also difficult in this case because of a strong chelating effect. Therefore, formation of a tetrahedral geometry around this carbon atom due to hydroxylation is extremely difficult. Because of this, hydroxylation of the triazine ring in **5** did not occur. Therefore, sufficient electrophilicity on the carbon atom and free movement of the attached uncoordinate pyridyl ring are the essential factors responsible for hydroxylation.

Conclusions

The present studies, therefore, demonstrated an unusual metal-induced hydroxylation of the triazine ring of a bridged tptz in dinuclear Ru(II) and Os(II) complexes. However, hydroxylation did not occur in the corresponding mononuclear complexes. Comparative studies revealed that sufficient electrophilicity upon the carbon atom and free movement of the attached pyridyl ring seems to be responsible for the hydroxylation reaction. The hydroxylated dinuclear complexes exist in two stereoisomeric forms, the *rac* form ($\Delta\Delta/\Lambda\Lambda$) and a *meso* form ($\Delta\Lambda/\Lambda\Delta$). Both diastereoisomers were separated and characterized on the basis of ^{1}H NMR data and single-crystal X-ray studies. To the best of our knowledge there is no other report of crystallographic characterization of a dinuclear Os(II) complex containing only polypyridyl ligands and also structural characterization of two diastereoisomeric forms of dinuclear complexes. The electrochemical studies revealed that there is a strong metal−metal electronic interaction mediated by the bridging ligand (tptz). The metal−metal communication occurs by an electron-transfer mode across the low-lying π^* orbital of the bridged tptz. The comproportionation constant (K_{com}) values of the mixed-valence species suggest that these dinuclear complexes belong to the Robin−Day type III class.

Acknowledgment. We are grateful to the Department of Science and Technology (DST), Government of India, for the financial support. A.K.B. gratefully acknowledges the CSIR for awarding a Senior Research Fellowship (SRF). Our sincere thanks to Dr. P. K. Ghosh, Director of this institute, and Dr. R. V. Jasra for their keen interest and encouragement. We also thank Dr. S. Muthusamy and Mr. P. Subramaniam for recording NMR spectra.

Supporting Information Available: A table of bond lengths and angles, figures shown spectra, and X-ray data, in CIF format. This material is available free of charge via the Internet at http://pubs.acs.org.

IC990938X